

Model of driven and decaying magnetic turbulence in a cylinder

Koen Kemel,^{1,2} Axel Brandenburg,^{1,2} and Hantao Ji³

¹*NORDITA, AlbaNova University Center, Roslagstullsbacken 23, SE-10691 Stockholm, Sweden*

²*Department of Astronomy, Stockholm University, SE 10691 Stockholm, Sweden*

³*Center for Magnetic Self-Organization in Laboratory and Astrophysical Plasmas, Princeton Plasma Physics Laboratory, Princeton University, Princeton, New Jersey 08543, USA*

(Received 6 June 2011; revised manuscript received 6 September 2011; published 21 November 2011)

Using mean-field theory, we compute the evolution of the magnetic field in a cylinder with outer perfectly conducting boundaries and imposed axial magnetic and electric fields. The thus injected magnetic helicity in the system can be redistributed by magnetic helicity fluxes down the gradient of the local current helicity of the small-scale magnetic field. A weak reversal of the axial magnetic field is found to be a consequence of the magnetic helicity flux in the system. Such fluxes are known to alleviate so-called catastrophic quenching of the α effect in astrophysical applications. A stronger field reversal can be obtained if there is also a significant kinetic α effect. Application to the reversed field pinch in plasma confinement devices is discussed.

DOI: [10.1103/PhysRevE.84.056407](https://doi.org/10.1103/PhysRevE.84.056407)

PACS number(s): 52.55.Lf, 52.55.Wq, 52.65.Kj, 96.60.qd

I. INTRODUCTION

The interaction created by a conducting medium moving at speed \mathbf{U} through a magnetic field \mathbf{B} is generally referred to as a dynamo effect. This effect plays important roles in astrophysics [1,2] and magnetospheric physics [3], as well as laboratory plasma physics [4]. It modifies the electric field in the rest frame, so that Ohm's law takes the form $\mathbf{J} = \sigma(\mathbf{E} + \mathbf{U} \times \mathbf{B})$, where \mathbf{J} is the current density, \mathbf{E} is the electric field, and σ is the conductivity. Of particular interest for the present paper is the case where an electric field \mathbf{E}^{ext} is induced through a transformer with a time-varying external magnetic field, \mathbf{B}^{ext} , as is the case in many plasma confinement experiments. Faraday's law gives $\partial \mathbf{B}^{\text{ext}} / \partial t = -\nabla \times \mathbf{E}^{\text{ext}}$, but unlike \mathbf{E}^{ext} , the magnetic field \mathbf{B}^{ext} is nonvanishing only within the transformer, i.e., outside the plasma. With such an externally induced electric field included, Ohm's law for the plasma becomes

$$\mathbf{J} = \sigma(\mathbf{E} + \mathbf{E}^{\text{ext}} + \mathbf{U} \times \mathbf{B}). \quad (1)$$

In a turbulent medium, often only averaged quantities (indicated below by overbars) are accessible. The averaged form of Ohm's law reads

$$\overline{\mathbf{J}} = \sigma(\overline{\mathbf{E}} + \overline{\mathbf{E}^{\text{ext}}} + \overline{\mathbf{U}} \times \overline{\mathbf{B}} + \overline{\mathcal{E}}), \quad (2)$$

where $\overline{\mathcal{E}} = \overline{\mathbf{u} \times \mathbf{b}}$ is referred to as the mean turbulent electromotive force, and $\mathbf{u} = \mathbf{U} - \overline{\mathbf{U}}$ and $\mathbf{b} = \mathbf{B} - \overline{\mathbf{B}}$ are fluctuations of velocity and magnetic field, respectively.

It has been known for some time that the averaged profiles, $\overline{\mathbf{J}}$ and $\sigma \overline{\mathbf{E}^{\text{ext}}}$ do not agree with each other in actual experiments. This disagreement cannot be explained by the $\overline{\mathbf{U}} \times \overline{\mathbf{B}}$ term either, leaving therefore $\overline{\mathcal{E}}$ as the only remaining term. Examples include the recent dynamo experiment in Cadarache [5] and in particular the reversed field pinch (RFP) [4,6,7], which is one of the configurations studied in connection with fusion plasmas. The name of this device derives from the fact that the toroidal (or axial, in a cylindrical geometry) magnetic field reverses sign near the periphery. Furthermore, in the astrophysical context it is well known that the $\overline{\mathcal{E}}$

term is responsible for the amplification and maintenance of large-scale magnetic fields [1,2].

The analogy among the various examples of the $\overline{\mathcal{E}}$ term has motivated comparative research between astrophysics and plasma physics applications [8]. In these cases, $\overline{\mathcal{E}}$ is found to have a component proportional to the mean field ($\alpha \overline{\mathbf{B}}$, referred to as the α effect) and a component proportional to the mean current density ($\eta_t \overline{\mathbf{J}}$, where η_t is the turbulent magnetic diffusivity). Since α is a pseudoscalar, one expects it to depend on the helicity of the flow, which is also a pseudoscalar. Decisive in developing the analogy between the α effects in astrophysics and laboratory plasma physics is the realization that α is caused not only by helicity in the flow (kinetic α effect), but also by the helicity of the magnetic field itself [9]. This magnetic contribution to the α effect has received increased astrophysical interest, because there are strong indications that such dynamos saturate by building up small-scale helical fields that lead to a magnetic α effect, which, in turn, counteracts the kinetic α effect [10–12]. This process can be described quantitatively by taking magnetic helicity evolution into account, which leads to what is known as the dynamical α quenching formalism that goes back to early work of Kleeeorin and Ruzmaikin [13]. However, it is now also believed that such quenching would lead to a catastrophically low saturation field strength [14], unless there are magnetic helicity fluxes inside or out of the domain. The divergence of such fluxes would limit the excessive build-up of small-scale helical fields [15]. This would reduce the magnetic α effect and thus allow the production of mean fields whose energy density is comparable to that of the kinetic energy of the turbulence [16].

These recent developments are purely theoretical, so the hope is that more can be learnt by applying the recently gained knowledge to experiments like the RFP [6,7]. Unlike tokamaks, the RFP is a relatively slender torus, so it makes sense to study its properties in a local model where one ignores curvature effects and considers a cylindrical piece of the torus. Along the axis of this cylinder there is a field-aligned current that makes the field helical. This field is susceptible to kink and tearing instabilities that lead to turbulence. It is generally believed that the resulting mean turbulent electromotive force

$\overline{\mathcal{E}}$ is responsible for the field reversal [4,17]. The turbulence is also believed to help driving the system toward a minimum energy state [18]. This state is nearly force-free and maintained by $\overline{\mathbf{E}}^{\text{ext}}$. This adds to the notion that the RFP must be sustained by some kind of dynamo process [19]. In Cartesian geometry a slow-down of turbulent decay has previously already been modeled using the dynamical quenching formalism [20].

The RFP has been studied extensively using three-dimensional simulations [19,21–23], which confirm the conjecture of J. B. Taylor [18] that the system approaches a minimum energy state. Additional understanding has been obtained using mean-field considerations [24,25]. Both here and in astrophysical dynamos there is an α effect that quantifies the correlation of the fluctuating parts of velocity and magnetic field. However, a major difference lies in the fact that in the RFP the α effect is caused by instabilities of the initially large-scale magnetic field, while in the astrophysical case one is concerned with the problem of explaining the origin of large-scale fields by the α effect [1,2]. However, this distinction may be too simplistic, and there is indeed evidence that in the RFP the α effect exists in close relation with a finite magnetic helicity flux [26], supporting the idea that so-called catastrophic quenching is avoided by helicity transport.

The purpose of this paper is to apply modern mean-field dynamo theory with dynamical quenching to a cylindrical configuration to allow a more meaningful comparison between the α effect in astrophysics and the one occurring in RFP experiments.

II. THE MODEL

To model the evolution of the magnetic field in a cylinder with imposed axial magnetic and electric fields, we employ mean-field theory, where the evolution of the mean field $\overline{\mathbf{B}}$ is governed by turbulent magnetic diffusivity and an α effect. Unlike the astrophysical case where α depends primarily on the kinetic helicity of the plasma, in turbulence from current-driven instabilities the α effect is likely to depend primarily on the current helicity of the small-scale field [9]. The current density is given by $\mathbf{J} = \nabla \times \mathbf{B}/\mu_0$, where μ_0 is the vacuum permeability, and the fluctuating current density is $\mathbf{j} = \nabla \times \mathbf{b}/\mu_0$. The mean current helicity density of the small-scale field is then given by $\overline{\mathbf{j} \cdot \mathbf{b}}$. To a good approximation, the $\overline{\mathbf{j} \cdot \mathbf{b}}$ term is proportional to the small-scale magnetic helicity density, $\overline{\mathbf{a} \cdot \mathbf{b}}$, where $\mathbf{a} = \nabla \times \overline{\mathbf{A}}$ is the vector potential of the fluctuating field. The generation of $\overline{\mathbf{a} \cdot \mathbf{b}}$ is coupled to the decay of $\overline{\mathbf{A} \cdot \mathbf{B}}$ through the magnetic helicity evolution equation [10, 11,13,27] such that $\overline{\mathbf{A} \cdot \mathbf{B}} + \overline{\mathbf{a} \cdot \mathbf{b}}$ evolves only resistively in the absence of magnetic helicity fluxes.

Note that $\overline{\mathbf{a} \cdot \mathbf{b}}$ is in general gauge dependent and might therefore not be a physically meaningful quantity. However, if there is sufficient scale separation, the mean magnetic helicity density of the fluctuating field can be expressed in terms of the density of field line linkages, which does not involve the magnetic vector potential and is therefore gauge independent [28]. For the large-scale field, on the other hand, the magnetic helicity density does remain in general gauge-dependent [29], but our final model will not be affected by this, because the

magnetic helicity of the large-scale magnetic field does not enter in the mean-field model.

We model an induced electric field by an externally applied electric field \mathbf{E}^{ext} . In the absence of any other induction effects this leads to a current density $\mathbf{J} = \sigma \mathbf{E}^{\text{ext}}$. Furthermore, we ignore a mean flow ($\overline{\mathbf{U}} = \mathbf{0}$) and assume that the velocity field has only a turbulent component \mathbf{u} . For simplicity we assume that $\overline{\mathbf{E}}^{\text{ext}}$ has no fluctuating part, i.e., $\mathbf{E}^{\text{ext}} = \overline{\mathbf{E}}^{\text{ext}}$. The decay of $\overline{\mathbf{B}}$ is accelerated by turbulent magnetic diffusivity η_t , which is expected to occur as a result of the turbulence connected with kink and tearing instabilities inherent to the RFP. This mean turbulent electromotive force has two components corresponding to the α effect and turbulent diffusion with

$$\overline{\mathcal{E}} = \alpha \overline{\mathbf{B}} - \eta_t \mu_0 \overline{\mathbf{J}}, \quad (3)$$

where we have ignored the fact that α and turbulent diffusivity are really tensors. The evolution equation for $\overline{\mathbf{B}}$ is then given by the mean-field induction equation,

$$\frac{\partial \overline{\mathbf{B}}}{\partial t} = \nabla \times (\alpha \overline{\mathbf{B}} - \eta_T \mu_0 \overline{\mathbf{J}} + \overline{\mathbf{E}}^{\text{ext}}), \quad (4)$$

where $\eta_T = \eta_t + \eta$ is the sum of turbulent and microscopic (Spitzer) magnetic diffusivities (not to be confused with the resistivity $\eta \mu_0$, which is also often called η). Note that only nonuniform and nonpotential contributions to $\overline{\mathbf{E}}^{\text{ext}}$ can have an effect.

As a starting point, we assume that the rms velocity u_{rms} and the typical wavenumber k_f of the turbulence are constant, although it is clear that these values should really depend on the level of the actual magnetic field. We estimate the value of η_t using a standard formula for isotropic turbulence,

$$\eta_t = \frac{1}{3} \tau \overline{u^2}, \quad (5)$$

where $\tau = (u_{\text{rms}} k_f)^{-1}$ is the correlation time of the turbulence and $u_{\text{rms}} = (\overline{u^2})^{1/2}$ is its rms velocity. Thus, we can also write $\eta_t = u_{\text{rms}}/3k_f$. The validity of Eq. (5) might be challenged by the fact that in simulations of hydromagnetic Taylor-Couette flows, measurements of η_t have suggested rather small values [30]. However, for helical magnetic fields, the roles of the α effect and turbulent magnetic diffusion are difficult to disentangle [11], and it is known that this can result in an apparent reduction of η_t [20].

We assume that α is given by the sum of a kinetic part, $\alpha_K = -\frac{1}{3} \tau \overline{\boldsymbol{\omega} \cdot \mathbf{u}}$, where $\boldsymbol{\omega} = \nabla \times \mathbf{u}$ is the vorticity, and a magnetic part, $\alpha_M = \frac{1}{3} \tau \overline{\mathbf{j} \cdot \mathbf{b}}/\rho_0$, where ρ_0 is the mean density of the plasma. Given that the turbulence is magnetically driven, our expectation is that α is determined entirely by the α_M term. Therefore we neglect this term in most cases, except for Sec. III C, where it will be included. Thus, we write [9]

$$\alpha = \alpha_K + \frac{1}{3} \tau \overline{\mathbf{j} \cdot \mathbf{b}}/\rho_0 \quad (6)$$

and use the fact that $\overline{\mathbf{j} \cdot \mathbf{b}}$ and $\overline{\mathbf{a} \cdot \mathbf{b}}$ are proportional to each other. For homogeneous turbulence we have $\overline{\mathbf{j} \cdot \mathbf{b}} = k_f^2 \overline{\mathbf{a} \cdot \mathbf{b}}/\mu_0$, although for inhomogeneous turbulence, $k_f^2 \overline{\mathbf{a} \cdot \mathbf{b}}/\mu_0$ has been found to be smaller than $\overline{\mathbf{j} \cdot \mathbf{b}}$ by a factor of two [31]. We compute the evolution of $\overline{\mathbf{a} \cdot \mathbf{b}}$ by considering first the evolution equation for $\overline{\mathbf{A} \cdot \mathbf{B}}$. Note that $\overline{\mathbf{A} \cdot \mathbf{B}}$ evolves

only resistively, unless there is material motion through the domain boundaries [29], so we have

$$\frac{d}{dt} \overline{\mathbf{A} \cdot \mathbf{B}} = 2\overline{\mathbf{E}^{\text{ext}} \cdot \mathbf{B}} - 2\eta\mu_0 \overline{\mathbf{J} \cdot \mathbf{B}} - \nabla \cdot \overline{\mathcal{F}}, \quad (7)$$

where $\overline{\mathcal{F}}$ is the mean magnetic helicity flux. While $\overline{\mathbf{B}}$ evolves subject to the mean field equation (4), the magnetic helicity of the mean field will change subject to the equation

$$\frac{d}{dt} (\overline{\mathbf{A} \cdot \mathbf{B}}) = 2\overline{\mathcal{E}^{\text{tot}} \cdot \mathbf{B}} - 2\eta\mu_0 \overline{\mathbf{J} \cdot \mathbf{B}} - \nabla \cdot \overline{\mathcal{F}}_m, \quad (8)$$

where $\overline{\mathcal{E}^{\text{tot}}} = \overline{\mathcal{E}} + \overline{\mathbf{E}^{\text{ext}}}$ and $\overline{\mathcal{F}}_m = \overline{\mathbf{E}} \times \overline{\mathbf{A}} + \overline{\Phi} \overline{\mathbf{B}}$ is the mean magnetic helicity flux from the mean magnetic field, and $\overline{\Phi}$ is the mean electrostatic potential. Here, $\overline{\mathbf{E}} = \eta\mu_0 \overline{\mathbf{J}} - \overline{\mathcal{E}^{\text{tot}}}$ is the mean electric field. Subtracting (8) from (7), we find a similar evolution equation for $\overline{\mathbf{a} \cdot \mathbf{b}}$,

$$\frac{d}{dt} \overline{\mathbf{a} \cdot \mathbf{b}} = -2\overline{\mathcal{E}} \cdot \overline{\mathbf{B}} - 2\eta\mu_0 \overline{\mathbf{j} \cdot \mathbf{b}} - \nabla \cdot \overline{\mathcal{F}}_f, \quad (9)$$

where $\overline{\mathcal{F}}_f = \overline{\mathcal{F}} - \overline{\mathcal{F}}_m$ is the mean magnetic helicity flux from the fluctuating magnetic field. Note that \mathbf{E}^{ext} does not enter in Eq. (9), because $\mathbf{E}^{\text{ext}} = \overline{\mathbf{E}^{\text{ext}}}$ has no fluctuations. This equation can readily be formulated as an evolution equation for α by writing $\alpha = (\tau k_f^2 / 3\rho_0\mu_0) \overline{\mathbf{a} \cdot \mathbf{b}}$, i.e.,

$$\frac{\partial \alpha}{\partial t} = -2\eta k_f^2 \overline{\mathcal{E}} \cdot \overline{\mathbf{B}} / B_{\text{eq}}^2 - 2\eta k_f^2 \alpha - \nabla \cdot \overline{\mathcal{F}}_\alpha, \quad (10)$$

where $\overline{\mathcal{F}}_\alpha = (\tau k_f^2 / 3\rho_0\mu_0) \overline{\mathcal{F}}_f$, which is a rescaled magnetic helicity flux of the small-scale field and B_{eq} is the field strength for which magnetic and kinetic energy densities are equal, i.e.,

$$B_{\text{eq}}^2 = \mu_0 \rho_0 u_{\text{rms}}^2 = (3\rho_0\mu_0/\tau) \eta_t. \quad (11)$$

We recall that in the astrophysical context, equation (10) is referred to as the dynamical quenching model [13,27]. In a first set of models we assume $\overline{\mathcal{F}}_\alpha = \mathbf{0}$, but later we shall allow for the fluxes to obey a Fickian diffusion law,

$$\overline{\mathcal{F}}_\alpha = -\kappa_\alpha \nabla \alpha, \quad (12)$$

where κ_α is a diffusion coefficient that is known to be comparable to or somewhat below the value of η_t [29,31].

We solve the governing equations (4) and (10) using the PENCIL CODE in cylindrical coordinates, (r, ϕ, z) , assuming axisymmetry and homogeneity along the z direction, $\partial/\partial\phi = \partial/\partial z = 0$, in a one-dimensional domain $0 \leq r \leq R$. On $r = 0$ regularity of all functions is obeyed, while on $r = R$ we assume perfect conductor boundary conditions, which implies that $\hat{\mathbf{n}} \times \overline{\mathbf{E}} = \hat{\mathbf{n}} \times \overline{\mathbf{J}} = \mathbf{0}$, and thus $\hat{\mathbf{n}} \times \partial \overline{\mathbf{A}} / \partial t = \mathbf{0}$, i.e., $\hat{\mathbf{n}} \times \overline{\mathbf{A}} = \text{const}$. Furthermore, we have $\alpha(R) = 0$, because on an impenetrable perfectly conducting boundary both kinetic and current helicities vanish.

As initial condition, we choose a uniform magnetic field B_0 in the z direction. In terms of the vector potential, this implies

$$\overline{\mathbf{A}}(r, 0) = (0, B_0 r / 2, 0) \quad (13)$$

for the initial value of $\overline{\mathbf{A}}(r, t)$. For the aforementioned perfect conductor boundary conditions, Eq. (13) implies $\overline{A}_\phi = B_0 R / 2$ and $\overline{A}_z = 0$ on $r = R$.

Following earlier work [32,33], we drive the system through the externally applied mean electromotive force in the z direction. Here we choose

$$\overline{E}_z^{\text{ext}}(r) = \overline{E}_0^{\text{ext}} J_0(k_1 r), \quad (14)$$

where $\overline{E}_0^{\text{ext}}$ is the value of the mean electromotive force on the axis and $k_1 R \approx 2.4048256$ is the rescaled cylindrical wavenumber for which $\overline{E}_z^{\text{ext}}(R) = 0$, which corresponds to the first zero of the Bessel function of order zero and thus satisfies the perfect conductor boundary condition on $r = R$. An important control parameter of our model is the nondimensional ratio

$$\mathcal{Q} = \overline{E}_0^{\text{ext}} / \eta_t k_f B_0, \quad (15)$$

which determines the degree of magnetic helicity injection. Other control parameters include the normalized strength of the imposed field,

$$\mathcal{B} = B_0 / B_{\text{eq}}, \quad (16)$$

and the value of the Lundquist number,

$$\mathcal{L} = v_A / \eta k_f, \quad (17)$$

which is a nondimensional measure of the inverse microscopic magnetic diffusivity, where $v_A = B_0 / \sqrt{\mu_0 \rho_0}$ is the Alfvén speed associated with the imposed field. The Lundquist number also characterizes the ratio of turbulent to microscopic magnetic diffusivity, i.e.,

$$\mathcal{R} \equiv \eta_t / \eta = u_{\text{rms}} / 3\eta k_f = \mathcal{L} / 3\mathcal{B}, \quad (18)$$

which we refer to as the magnetic Reynolds number. Note that, if we were to define the magnetic Reynolds number as $R_m = u_{\text{rms}} / \eta k_f$, as is often done, then $\mathcal{R} = R_m / 3$ would be three times smaller. Finally, the wavenumber of the energy-carrying turbulent eddies is expressed in terms of the dimensionless value of $k_f R$. We treat k_f as an adjustable parameter that characterizes the degree of scale separation, i.e., the ratio of the scale of the domain to the characteristic scale of the turbulence. In most of the cases we consider $k_f R = 10$. In summary, our model is characterized by four parameters: \mathcal{Q} , \mathcal{B} , \mathcal{L} , and $k_f R$. In models with magnetic helicity flux we also have the parameter $\tilde{\kappa}_\alpha \equiv \kappa_\alpha / \eta_t$, where the tilde indicates nondimensionalization. In models with a kinetic α effect, there is yet another coefficient that will be specified later.

In addition to plotting the resulting profiles of magnetic field and current density, we also determine mean-field magnetic energy and helicity, as well as mean-field current helicity, i.e.,

$$M_m = \langle \overline{\mathbf{B}}^2 / 2\mu_0 \rangle, \quad H_m = \langle \overline{\mathbf{A}} \cdot \overline{\mathbf{B}} \rangle, \quad C_m = \langle \overline{\mathbf{J}} \cdot \overline{\mathbf{B}} \rangle, \quad (19)$$

where $\langle \cdot \rangle = \int_0^R \cdot r dr / (\frac{1}{2} R^2)$ denotes a volume average, and the subscript m refers to mean-field quantities. Following similar practice of earlier work [11,34], we characterize the solutions further by computing the effective wavenumber of the mean field, k_m , and the degree ϵ_m to which it is helical, via

$$k_m^2 = \mu_0 C_m / H_m, \quad \epsilon_m = C_m / 2k_m M_m. \quad (20)$$

In the following we shall refer to ϵ_m as the relative magnetic helicity. We recall that, even though $\overline{\mathbf{A}} \cdot \overline{\mathbf{B}}$ is gauge dependent, for perfect conductor boundary conditions, the integral

TABLE I. \mathcal{Q} dependence of k_m and ϵ_m for $\mathcal{B} = 1$, $\mathcal{L} = 1000$, and $k_f R = 10$.

\mathcal{Q}	0.01	0.03	0.10	0.20	0.50	1.00
$k_m R$	2.76	3.44	4.63	5.26	6.49	7.20
ϵ_m	0.95	0.91	0.84	0.82	0.78	0.73

$\int \overline{\mathbf{A}} \cdot \overline{\mathbf{B}} dV$ is gauge invariant, and so is then k_m . Similar definitions also apply to the fluctuating field, whose current helicity is given by

$$C_f = \langle \alpha \rangle B_{\text{eq}}^2 / \mu_0 \eta_t. \quad (21)$$

The magnetic helicity of the fluctuating field is then $H_f = \mu_0 C_f / k_f^2$. The magnetic energy of the fluctuating field can be estimated under the assumption that the field is fully helical, i.e., $\langle \mathbf{b}^2 \rangle = k_f |\langle \mathbf{a} \cdot \mathbf{b} \rangle|$, so that $M_f = |C_f| / 2k_f$. We study both the steady state case where \mathcal{Q} and \mathcal{B} are nonvanishing, and the decaying case where $\mathcal{Q} = \mathcal{B} = 0$. In the latter case, we monitor the decay rates of the magnetic field.

III. RESULTS

A. Driven field-aligned currents

We begin by considering the case without magnetic helicity fluxes and take $\mathcal{B} = 1$, $\mathcal{L} = 1000$ (corresponding to $\mathcal{R} = 333$), and $k_f R = 10$. The resulting values of k_m and ϵ_m are given in Table I, and the mean magnetic field profiles are compared in Fig. 1 for different values of \mathcal{Q} . It turns out that, as we increase the value of \mathcal{Q} , the magnetic helicity of the mean field increases, i.e., the product $\epsilon_m k_m$ increases, but the *relative*

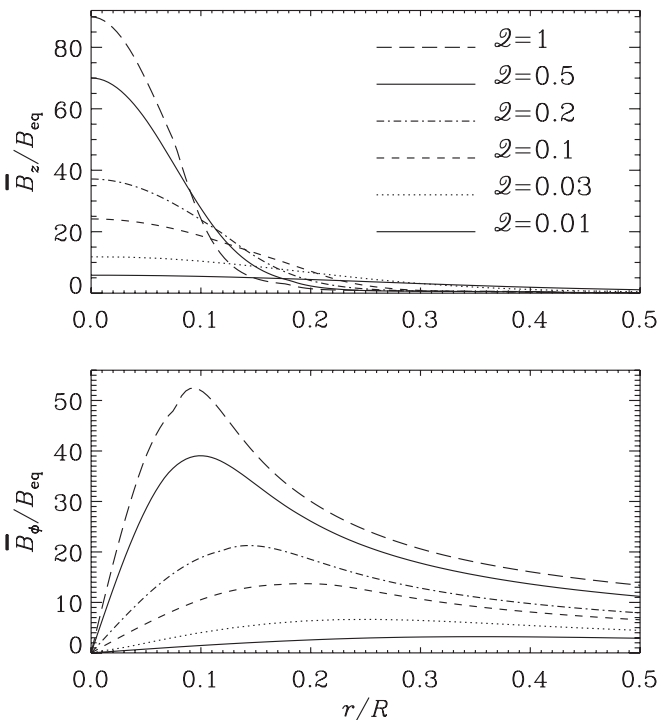

 FIG. 1. Equilibrium profiles for three different driving strengths for $\mathcal{B} = 1$, $\mathcal{L} = 1000$, and $k_f R = 10$.

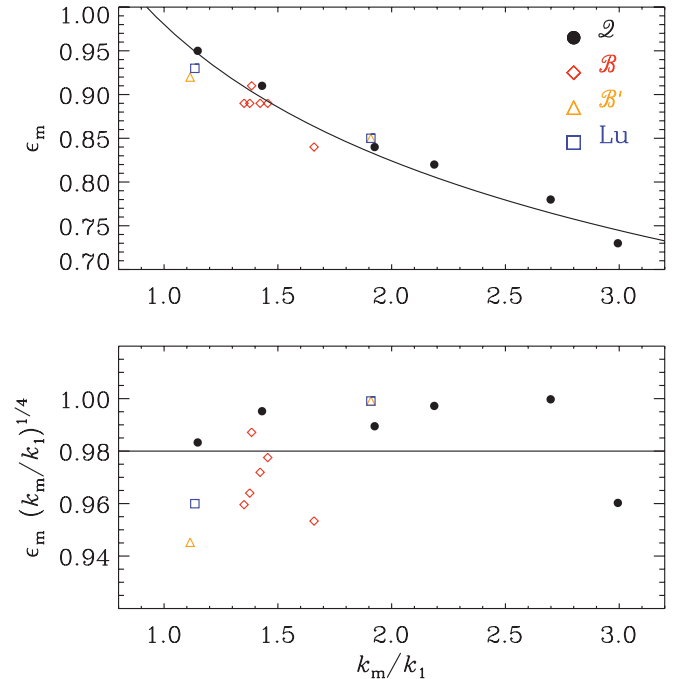
 TABLE II. \mathcal{B} dependence of k_m and ϵ_m for $\mathcal{Q} = 0.1$, $\mathcal{R} = 100$, and $k_f R = 10$.

\mathcal{B}	0.1	0.2	0.5	1	2	5	10
$k_m R$	1.80	3.33	3.50	3.99	3.42	3.31	3.25
ϵ_m	0.51	0.91	0.89	0.84	0.89	0.89	0.89

helicity of the mean magnetic field decreases slightly, i.e., ϵ_m decreases. The value of k_m increases with \mathcal{Q} , which means that the mean field will be confined to a progressively thinner core around the axis. Furthermore, the anticorrelation between ϵ_m and k_m is also found when varying \mathcal{B} (see Table II), \mathcal{L} , or \mathcal{R} . This is demonstrated in Fig. 2, where we show that ϵ_m is in fact proportional to $(k_m/k_1)^{-1/4}$ and that the product $\epsilon_m (k_m/k_1)^{1/4}$ is approximately constant, even though \mathcal{Q} , \mathcal{B} , or \mathcal{L} is varied. This scaling is unexpected, and there is currently no theoretical interpretation for this behavior.

It is interesting to note that k_m does not vary significantly with \mathcal{B} , provided \mathcal{R} is held fixed. However, for weak fields, e.g., for $\mathcal{B} = 0.1$, the dynamics of the mean field are no longer controlled by magnetic helicity evolution, and the value of $k_m R$ has then dropped suddenly by nearly a factor of 2, and ϵ_m is in that case no longer anticorrelated with k_m . This data point falls outside the plot range of Fig. 2 and is therefore not included. Also, if only \mathcal{L} is held fixed, so that \mathcal{R} varies with \mathcal{B} , then k_m is no longer weakly varying with \mathcal{B} , and varies more strongly in that case.

We must ask ourselves why the axial field component does not show a reversal in radius, as is the case in the RFP. Experimental studies of the RFP provide direct evidence for


 FIG. 2. (Color online) Dependence of ϵ_m on k_m for different sets of runs where either \mathcal{Q} is varied (filled symbols), \mathcal{B} is varied while keeping $\mathcal{R} = 100$ (red diamonds), \mathcal{B} is varied while keeping $\mathcal{L} = 100$ (orange triangles), or \mathcal{L} is varied (blue squares).

a reversal. By comparing radial profiles of the axial current, \bar{J}_\parallel/σ , with those of the axial electric field, \bar{E}_\parallel , one concludes that the mismatch between the two must come from the $\bar{\mathcal{E}}_\parallel$ term [17,35]. These studies show that $\bar{E}_\parallel < \bar{J}_\parallel/\sigma$ near the axis and $\bar{E}_\parallel > \bar{J}_\parallel/\sigma$ away from it (assuming $\bar{B}_\parallel > 0$ on the axis). Comparing with Eq. (2), it is therefore clear that $\bar{\mathcal{E}}_\parallel$ must then be negative near the axis and positive near the outer rim. Turning now to dynamo theory, it should be emphasized that there are two contributions to $\bar{\mathcal{E}}_\parallel$, one from $\alpha\bar{\mathbf{B}}$ and one from $-\eta_t\mu_0\bar{\mathbf{J}}$; see Eq. (3). Let us therefore discuss in the following the expected sign of $\bar{\mathcal{E}}_\parallel$. Given that \mathcal{Q} is positive, $\bar{\mathbf{J}} \cdot \bar{\mathbf{B}}$ must also be positive, and therefore we expect α to be positive. If the mean magnetic field were to correspond to that of a growing dynamo, the α term would dominate over the η_t term, but this is likely not the case here where the field is either statistically steady or decaying. Indeed, by manipulating Eq. (10) we see that, in the steady state without magnetic helicity fluxes, the equation for α takes the form

$$\alpha = \frac{\mathcal{R}\eta_t\mu_0\bar{\mathbf{J}} \cdot \bar{\mathbf{B}}/B_{\text{eq}}^2}{1 + \mathcal{R}\bar{\mathbf{B}}^2/B_{\text{eq}}^2}, \quad (22)$$

see, e.g., Ref. [11]. However, as alluded to above, the relevant term entering $\bar{\mathcal{E}}$ is the combination $\alpha_{\text{red}} = \alpha - \eta_t\mu_0\bar{\mathbf{J}} \cdot \bar{\mathbf{B}}/B_{\text{eq}}^2$, which is the reduced α . Inserting Eq. (22) yields

$$\alpha_{\text{red}} = -\frac{\eta_t\mu_0\bar{\mathbf{J}} \cdot \bar{\mathbf{B}}/B_{\text{eq}}^2}{1 + \mathcal{R}\bar{\mathbf{B}}^2/B_{\text{eq}}^2}, \quad (23)$$

with a minus sign in front. The important point here is that α_{red} is indeed negative if $\bar{\mathbf{J}} \cdot \bar{\mathbf{B}}$ is positive. This means that we can only expect $\bar{E}_\parallel < \bar{J}_\parallel/\sigma$, which is the situation in the RFP near the axis [35]. In order to reverse the ordering and to produce a reversal of the axial field, one would need to have an α effect that dominates over turbulent diffusion. Note also that for strong mean fields, α_{red} is of the order of the microscopic magnetic diffusivity. (This situation is well known for nonlinear dynamos, because there α_{red} and the microscopic diffusion term η_{k_m} have to balance each other in a steady state [36].)

We note in passing that k_f enters neither in Eq. (22) nor in Eq. (23). This is the reason why we have not performed a detailed parameter study with respect to $k_f R$. However, k_f does enter if there is a magnetic helicity flux and it affects the time-dependent case, as is also clear from Eq. (10). Both cases will be considered below.

B. Effect of magnetic helicity flux

Next, we study cases where a diffusive magnetic helicity flux is included. In our model with perfectly conducting boundaries, the magnetic helicity flux vanishes on the boundaries, so no magnetic helicity is exported from the domain, but the divergence of the flux is finite and can thus modify the magnetic α effect. The same is true for periodic boundaries, where no magnetic helicity is exported, but the flux divergence is finite and can alleviate catastrophic quenching in dynamos driven by the kinetic α effect [37].

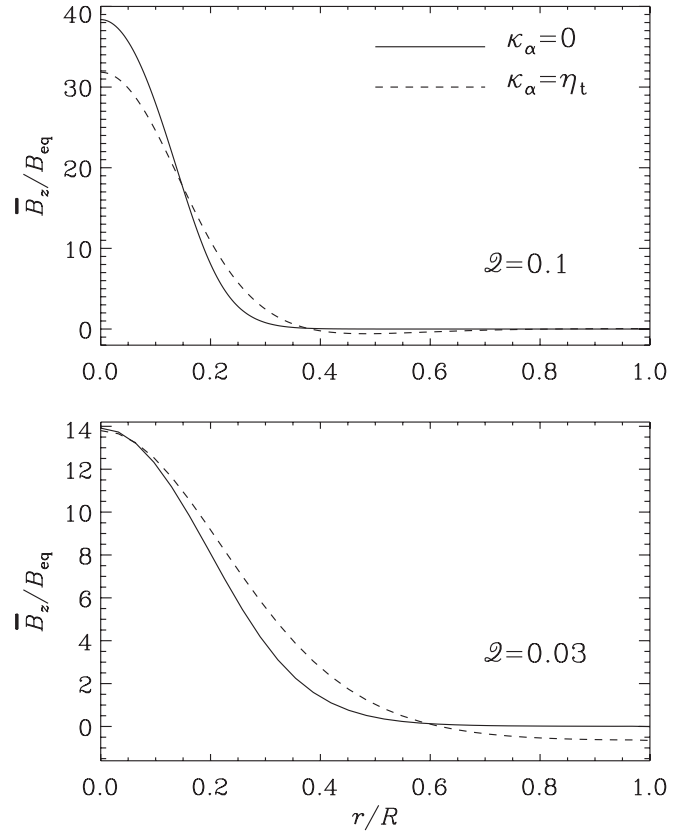


FIG. 3. Effect of magnetic helicity flux on equilibrium profiles of \bar{B}_z for $\mathcal{Q} = 0.1$ (upper panel) and $\mathcal{Q} = 0.03$ (lower panel). In both cases we have $B = 1$, $\mathcal{L} = 1000$, and $k_f R = 10$. Note the field reversal at the outer rim in the latter case.

In Fig. 3 we compare profiles of \bar{B}_z with and without magnetic helicity flux. It turns out that the κ_α term has the effect of making the resulting profile of \bar{B}_z less steep. More interestingly, it can lead to a reversal of \bar{B}_z at intermediate radii. For our reference run with $\mathcal{Q} = 0.1$ (upper panel), the reversal is virtually absent at the rim of the cylinder. This is mainly because the pinch is so narrow; see Table III. However, when decreasing \mathcal{Q} to 0.03, there is a clear reversal also at the outer rim (lower panel). On the other hand, decreasing \mathcal{Q} to 0.01 does not increase the extent of the reversal. In none of these cases the field reversal is connected with a change of sign of α_{red} . Instead, α_{red} is always found to be negative, even in the presence of a magnetic helicity flux. The sign reversal of \bar{B}_z is therefore associated with a sign reversal of \bar{J}_z at the same radius. Nevertheless, the reversal is still not very strong with $\min(\bar{B}_z)/\max(\bar{B}_z) \approx -0.07$, while in laboratory RFPs this ratio is typically -0.2 [35].

TABLE III. Values of k_m and ϵ_m with and without magnetic helicity flux for $B = 1$, $\mathcal{L} = 1000$, and $k_f R = 10$.

\mathcal{Q}	0.03		0.1	
	$\kappa_\alpha/\eta_t = 0$	$\kappa_\alpha/\eta_t = 1$	$\kappa_\alpha/\eta_t = 0$	$\kappa_\alpha/\eta_t = 1$
$k_m R$	4.63	4.50	3.51	3.32
ϵ_m	0.84	0.83	0.91	0.92

C. Enhancing the reversal through a kinetic α effect

The models presented above have shown that a reversal of \overline{B}_z is only possible when there is a diffusive magnetic helicity flux within the domain. This raises the question whether this phenomenon is more general and whether it also occurs when one tries to promote a reversal through an imposed kinetic α effect.

We have already seen that the weak reversal discussed in Sec. III B was connected neither with a sign reversal of α nor with one of α_{red} . It might therefore be illuminating to impose a kinetic α effect with a sign reversal, given by

$$\alpha_K = \alpha_{K0} J_0(k_\alpha r), \quad (24)$$

where $k_\alpha \approx 5.5200781$ corresponds to the second zero of J_0 , thus obeying $\alpha_K(R) = 0$. It turns out that it is now indeed possible to enhance the reversal discussed above significantly, provided α_{K0} is negative. This is shown in Fig. 4, where we compare profiles of \overline{B}_z for $\alpha_{K0} \equiv \alpha_{K0} R/\eta_t = 0, 10,$ and 30 . Here, the tilde denotes nondimensionalization. In the upper panel we keep $\tilde{\kappa}_\alpha \equiv \kappa_\alpha/\eta_t = 1$, but in the lower panel it is varied and takes the values $0, 0.3,$ and 1 . The results show quite clearly that a strong field reversal is only possible if there is a significant diffusive magnetic helicity flux within the domain.

To understand the reason for the enhancement of the reversal in the presence of a kinetic α effect and a magnetic

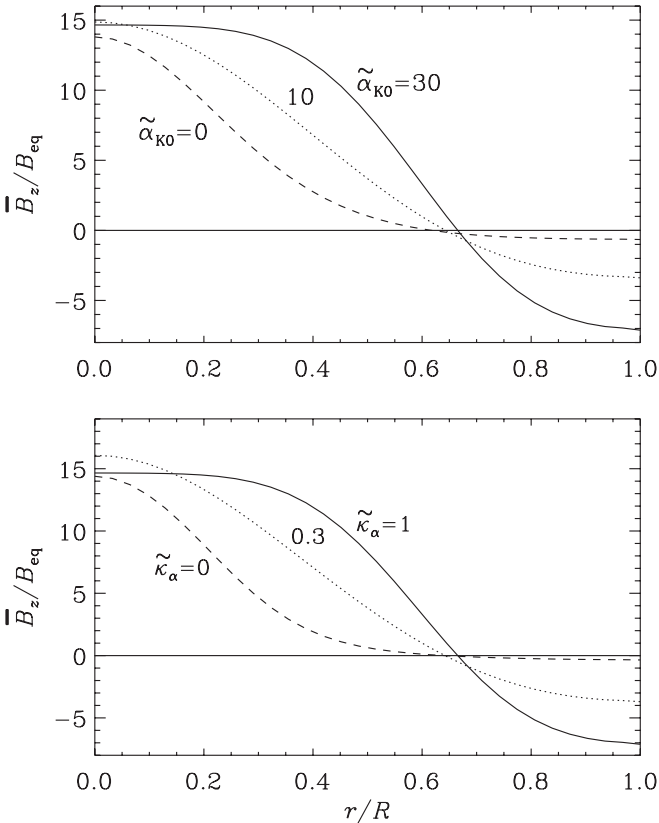


FIG. 4. Profiles of \overline{B}_z for $\alpha_{K0} = 0, 10,$ and 30 with $\tilde{\kappa}_\alpha = 1$ (upper panel), and $\tilde{\kappa}_\alpha = 0, 0.3,$ and 1 with $\alpha_{K0} = 30$ (lower panel), using $Q = 0.03$ in both cases.

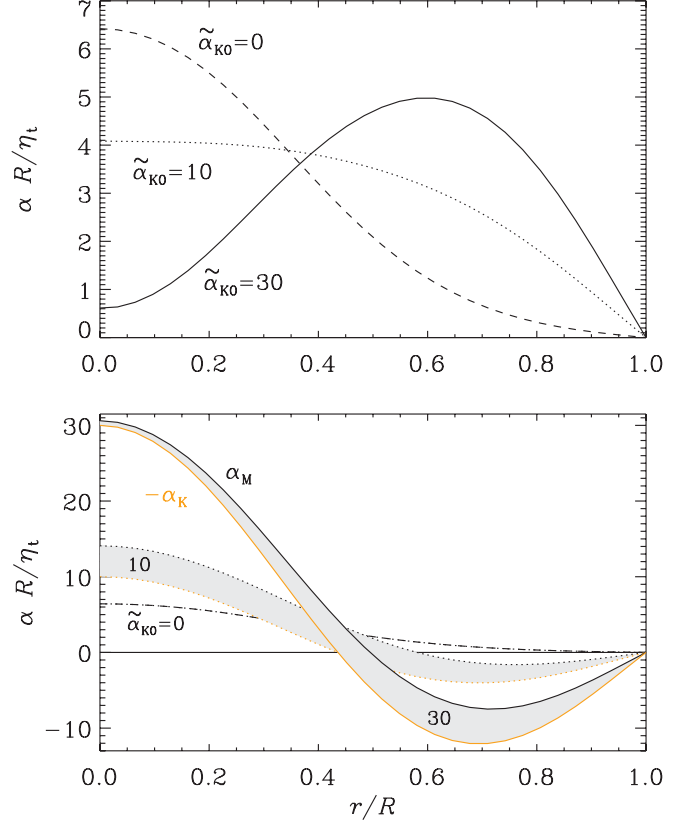


FIG. 5. (Color online) Profiles of α (upper panel) and α_M together with $-\alpha_K$ (lower panel) for $\alpha_{K0} = 0, 10,$ and 30 with $\tilde{\kappa}_\alpha = 1$ and $Q = 0.03, \mathcal{B} = 1, \mathcal{L} = 1000,$ and $k_f R = 10$. The difference between α_M and $-\alpha_K$ (gray-shaded area) corresponds to α .

helicity flux, we need to consider the resulting profiles of $\alpha = \alpha_K + \alpha_M$. For $\alpha_{K0} = 0$, we have a positive maximum of α at $r = 0$. Adopting now negative values of α_{K0} , we find that α is decreased at $r = 0$, because α_M and α_K have here opposite signs. At larger radii ($r/R > 0.5$), α is enhanced for larger values of α_{K0} , leading to a shift of its maximum away from the axis. Nevertheless, α remains strictly positive; see the upper panel of Fig. 5. This means that the sign change of α_K has actually induced a sign change of α_M ; see the lower panel of Fig. 5. This, in turn, suggests that the current helicities of large-scale and small-scale fields have also changed, which is indeed compatible with our result that \overline{J}_z remains positive, but \overline{B}_z becomes negative for $r/R \gtrsim 0.5$. Thus, the field reversal may be linked to the tendency of α to maintain always the same sign. This is further supported by the fact that a diffusive magnetic helicity flux also tends to minimize spatial variations of α .

The addition of a kinetic α effect can be motivated by the fact that even purely magnetically driven turbulence will produce flows with kinetic helicity and will thus lead to an α_K term, although we expect it to be weaker than the magnetic term so as not to produce dynamo action in the absence of external driving. To determine the critical value of α_{K0} for self-excited dynamo action, we put $Q = \mathcal{B} = 0$ and find that for $-\alpha_{K0} R/\eta_t > 11.49$ the dynamo is self-excited.

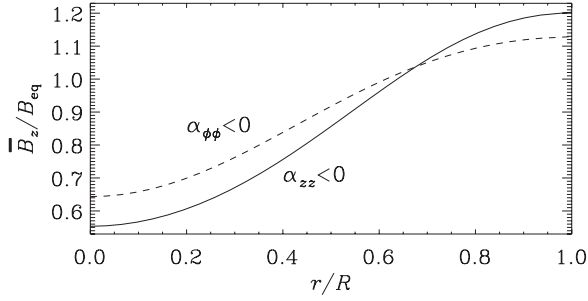


FIG. 6. Profiles of \bar{B}_z for $\alpha = \text{diag}(0, -0.2, 1)\alpha_M$ (dashed line) and another with $\alpha = \text{diag}(0, 1, -0.2)\alpha_M$ (solid line), using $Q = 0.03$, $B = 1$, $\mathcal{L} = 1000$, $k_f R = 10$, and $\kappa_\alpha = \eta_t$.

D. Anisotropy of α

So far we have completely ignored the fact that α and turbulent magnetic diffusivity are really tensors. In fact, recent calculation of current-driven instabilities in Couette flows suggest that the two nonradial diagonal components of α_{ij} have opposite signs [38]. It is unclear whether this result is specific to the presence of differential rotation. Nevertheless, it is important to assess the sensitivity of our results to changes in the sign of the two diagonal components, $\alpha_{\phi\phi}$ and α_{zz} .

We perform experiments for a case with $\alpha = \text{diag}(0, -0.2, 1)\alpha_M$ and another with $\alpha = \text{diag}(0, 1, -0.2)\alpha_M$, using $Q = 0.03$, $B = 1$, $\mathcal{L} = 1000$, $k_f R = 10$, and $\kappa_\alpha = \eta_t$. In both cases, \bar{B}_z increases away from the axis (Fig. 6), which has never been seen in actual RFP experiments. On the other hand, we must keep in mind that opposite signs of $\alpha_{\phi\phi}$ and α_{zz} have mainly been inferred for Couette flows, while in the RFP there is no systematic rotation. Also, of course, the determination of α may be contaminated by ill-determined coefficients of the turbulent magnetic diffusivity tensor. It would therefore be important to revisit this issue in future simulations of the RFP.

E. Decay calculations

Next, we consider the case of a decaying magnetic field in the absence of an external electric field. In that case all components of $\bar{\mathbf{B}}$ must eventually decay to zero. The evolution of the magnetic energy of the resulting mean and fluctuating fields is shown in Fig. 7, together with the evolution of k_m and ϵ_m . At early times, when $\langle \bar{\mathbf{B}}^2 \rangle \gg B_{\text{eq}}^2$, the energy of the large-scale magnetic field decays at the resistive rate $\lambda = -2\eta k_m^2$. During that time, the energy of the small-scale field stays approximately constant: The magnetically generated α effect almost exactly balances turbulent diffusion and the magnetic field can only decay at the resistive rate. However, at later times, when $\langle \bar{\mathbf{B}}^2 \rangle \ll B_{\text{eq}}^2$, the energy of the small-scale field decays with a negative growth rate $\lambda = -2\eta k_m^2$, which then speeds up the decay of the energy of the large-scale magnetic field to a rate that is about $1.3 \times \eta_t k_m^2$, where we have used the value $k_m R = 3.1$ that is relevant for the late-time decay. This value is also that obeying Taylor's [18] postulated minimum energy state. Again, no reversal of the magnetic field is found, except in cases where there is an internal magnetic helicity flux in the system.

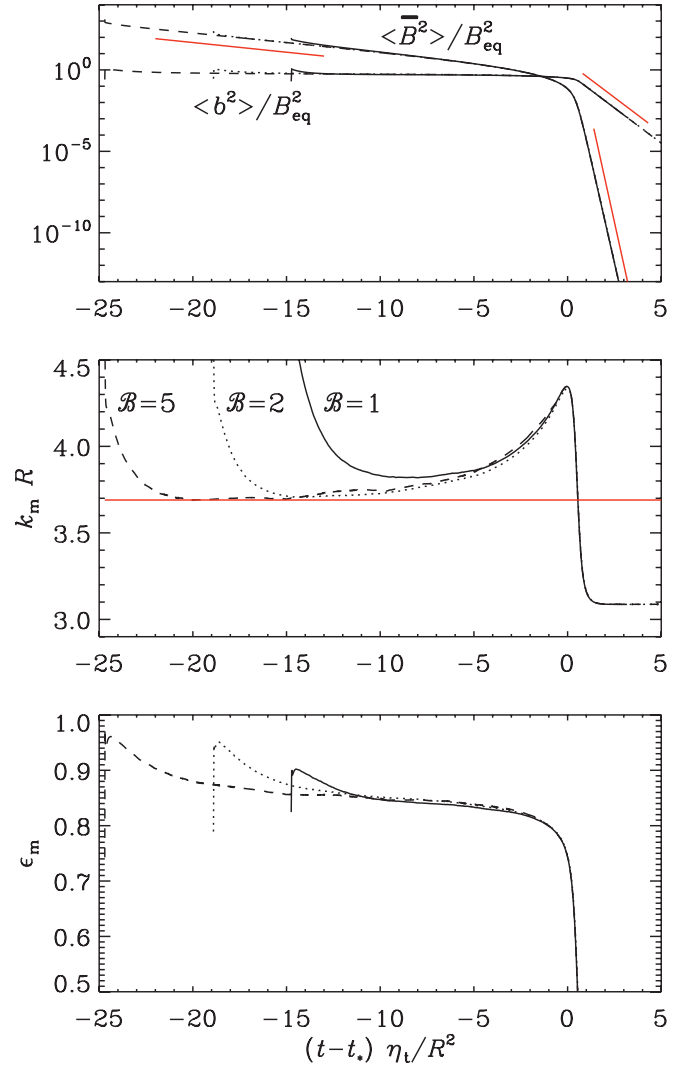


FIG. 7. (Color online) Evolution of $\langle \bar{\mathbf{B}}^2 \rangle / B_{\text{eq}}^2$, k_m/k_1 , and ϵ_m for different values of B . Note that time is shifted by t_* , which is the time when k_m attains its second maximum. In the top panel, the red lines indicate resistive decay rate of the large-scale field at early times, resistive decay rate of the small-scale field at late times, and the turbulent decay rate of the large-scale field at late times.

IV. CONCLUSIONS

The present work is an application of the dynamical quenching model of modern mean-field dynamo theory to magnetically driven and decaying turbulence in cylindrical geometry. In the driven case, an external electric field is applied, which leads to magnetic helicity injection at large scales. Such a situation has not yet been considered in the framework of mean-field theory. It turns out that in such a case there is a weak anticorrelation between the actual value of magnetic helicity of the mean field, $\epsilon_m k_m$, and the relative magnetic helicity ϵ_m with $\epsilon_m \sim k_m^{-1/4}$. This weak anticorrelation is found to be independent of whether Q , B , or \mathcal{L} are varied. No theoretical interpretation of this behavior has yet been offered. In the decaying case, we find that the decay rate is close to the (microscopic) resistive value when the field is strong, i.e., $|\bar{\mathbf{B}}| > B_{\text{eq}}$, and drops to the turbulent resistive

value when the mean field becomes weaker. This behavior has also been found in earlier calculation of the decay of helical magnetic fields in Cartesian geometry [20].

The original anticipation was that our model reproduces some features of the RFP that is studied in connection with fusion plasma confinement. It turns out that the expected field reversal that gives the RFP its name is found to require the presence of magnetic helicity fluxes. Without such fluxes, there is no reversal; see Fig. 3. Nevertheless, the reversal is rather weak compared with laboratory RFPs. This discrepancy can have several reasons. On the one hand, we have been working here with a model that has previously been tested only under simplifying circumstances in which there is turbulent dynamo action driven by kinetic helicity supply. It is therefore possible that the model has shortcomings that have not yet been fully understood. A related possibility is that the model is basically valid, but our application to the RFP has been too crude. For example, the assumption of fixed values of η_t and B_{eq} is certainly quite simplistic. On the other hand, it is not clear that this simplification would really affect the outcome of the model in any decisive way. A different possibility is that the application of an external electric field is not representative of the RFP. Yet another possibility is that the α effect is boosted by a kinetic contribution. If this is indeed the case, there would be particular requirements for such an α : it must be negative near the axis (for positive current helicity of the large-scale field), but of opposite sign in the outer parts. Such an α effect has

not yet been derived or otherwise motivated for such systems. However, if such an effect is present, it should be possible to measure it from future direct numerical simulations of such systems.

One of the remarkable predictions from our model is that, regardless of whether or not a kinetic α effect is present, magnetic helicity fluxes within the domain are always necessary for a reversal. This is indeed compatible with measurements from RFP experiments [4], where transport of magnetic helicity from one part of the plasma to another has been observed. Thus, our simple model has a number of detailed properties that can be tested by performing corresponding three-dimensional simulations of a similar setup. This has not yet been attempted, but it would clearly constitute a natural next step to take.

ACKNOWLEDGMENTS

We thank two anonymous reviewers for their comments and suggestions that have led to additional calculations presented now in the paper. This work was supported in part by the Swedish Research Council, Grant 621-2007-4064, the European Research Council under the AstroDyn Research Project 227952, and the National Science Foundation under Grant No. NSF PHY05-51164. HJ acknowledges support from the US Department of Energy's Office of Science-Fusion Energy Sciences Program under Contract Number DE-AC02-09CH11466.

-
- [1] H. K. Moffatt, *Magnetic Field Generation in Electrically Conducting Fluids* (Cambridge University Press, Cambridge, UK, 1978).
 - [2] F. Krause and K.-H. Rädler, *Mean-Field Magnetohydrodynamics and Dynamo Theory* (Pergamon Press, Oxford, 1980).
 - [3] T. Ogino, *J. Geophys. Res.* **91**, 6791 (1986).
 - [4] H. Ji, S. C. Prager, A. F. Almagri, J. S. Sarff, and H. Toyama, *Phys. Plasmas* **3**, 1935 (1996).
 - [5] R. Monchaux *et al.*, *Phys. Rev. Lett.* **98**, 044502 (2007).
 - [6] H. A. B. Bodin and A. A. Newton, *Nuclear Fusion* **20**, 1255 (1980).
 - [7] J. B. Taylor, *Phys. Rev. Lett.* **58**, 741 (1986).
 - [8] E. G. Blackman and H. Ji, *Mon. Not. R. Astron. Soc.* **369**, 1837 (2006).
 - [9] A. Pouquet, U. Frisch, and J. Léorat, *J. Fluid Mech.* **77**, 321 (1976).
 - [10] G. B. Field and E. G. Blackman, *Astrophys. J.* **572**, 685 (2002).
 - [11] E. G. Blackman and A. Brandenburg, *Astrophys. J.* **579**, 359 (2002).
 - [12] K. Subramanian, *Bull. Astr. Soc. India* **30**, 715 (2002).
 - [13] N. I. Kleeorin and A. A. Ruzmaikin, *Magnetohydrodynamics* **18**, 116 (1982).
 - [14] A. Brandenburg and K. Subramanian, *Astron. Nachr.* **326**, 400 (2005).
 - [15] A. Brandenburg and C. Sandin, *Astron. Astrophys.* **427**, 13 (2004).
 - [16] A. Brandenburg, *Astrophys. J.* **625**, 539 (2005).
 - [17] H. Ji and S. C. Prager, *Magnetohydrodynamics* **38**, 191 (2002); e-print [arXiv:astro-ph/0110352](https://arxiv.org/abs/astro-ph/0110352).
 - [18] J. B. Taylor, *Phys. Rev. Lett.* **33**, 1139 (1974).
 - [19] A. Y. Aydemir and D. C. Barnes, *Phys. Rev. Lett.* **52**, 930 (1984).
 - [20] T. A. Yousef, A. Brandenburg, and G. Rüdiger, *Astron. Astrophys.* **411**, 321 (2003).
 - [21] D. D. Schnack, E. J. Caramana, and R. A. Nebel, *Phys. Fluids* **28**, 321 (1985).
 - [22] H.-E. Sætherblom, S. Mazur, and P. Nordlund, *Plasmas Phys. Contr. Fusion* **38**, 2205 (1996).
 - [23] S. Cappello, D. Bonfiglio, and D. F. Escande, *Phys. Plasmas* **13**, 056102 (2006).
 - [24] H. R. Strauss, *Phys. Fluids* **28**, 2786 (1985).
 - [25] A. Bhattacharjee and E. Hameiri, *Phys. Rev. Lett.* **57**, 206 (1986).
 - [26] H. Ji, *Phys. Rev. Lett.* **83**, 3198 (1999).
 - [27] N. Kleeorin, I. Rogachevskii, and A. Ruzmaikin, *Astron. Astrophys.* **297**, 159 (1995).
 - [28] K. Subramanian and A. Brandenburg, *Astrophys. J.* **648**, L71 (2006).
 - [29] A. Hubbard and A. Brandenburg, *Geophys. Astrophys. Fluid Dyn.* **104**, 577 (2010).
 - [30] M. Gellert and G. Rüdiger, *Phys. Rev. E* **80**, 046314 (2009).
 - [31] D. Mitra, S. Candelaresi, P. Chatterjee, R. Tavakol, and A. Brandenburg, *Astron. Nachr.* **331**, 130 (2010).
 - [32] C. R. Sovinec and S. C. Prager, *Nucl. Fusion* **39**, 777 (1999).

- [33] J.-E. Dahlin and J. Scheffel, *Nucl. Fusion* **47**, 9 (2007).
- [34] A. Brandenburg, W. Dobler, and K. Subramanian, *Astron. Nachr.* **323**, 99 (2002).
- [35] Y. L. Ho, S. C. Prager, and D. D. Schnack, *Phys. Rev. Lett.* **62**, 1504 (1989).
- [36] A. Brandenburg, K.-H. Rädler, M. Rheinhardt, and K. Subramanian, *Astrophys. J.* **676**, 740 (2008).
- [37] A. Hubbard and A. Brandenburg, *Astrophys. J.* **727**, 11 (2011).
- [38] M. Gellert, G. Rüdiger, and R. Hollerbach, *Mon. Not. R. Astron. Soc.* **414**, 2696 (2011).